

## ARTICLE

# The *CFTR* frameshift mutation 3905insT and its effect at transcript and protein level

Javier Sanz<sup>1</sup>, Thomas von Känel<sup>1</sup>, Mircea Schneider<sup>1</sup>, Bernhard Steiner<sup>2</sup>, André Schaller<sup>1</sup> and Sabina Gallati<sup>\*1</sup>

Cystic fibrosis (CF) is one of the most common genetic diseases in the Caucasian population and is characterized by chronic obstructive pulmonary disease, exocrine pancreatic insufficiency, and elevation of sodium and chloride concentrations in the sweat and infertility in men. The disease is caused by mutations in the CF transmembrane conductance regulator (*CFTR*) gene, which encodes a protein that functions as chloride channel at the apical membrane of different epithelia. Owing to the high genotypic and phenotypic disease heterogeneity, effects and consequences of the majority of the *CFTR* mutations have not yet been studied. Recently, the frameshift mutation 3905insT was identified as the second most frequent mutation in the Swiss population and found to be associated with a severe phenotype. The frameshift mutation produces a premature termination codon (PTC) in exon 20, and transcripts bearing this PTC are potential targets for degradation through nonsense-mediated mRNA decay (NMD) and/or for exon skipping through nonsense-associated alternative splicing (NAS). Using RT-PCR analysis in lymphocytes and different tissue types from patients carrying the mutation, we showed that the PTC introduced by the mutation does neither elicit a degradation of the mRNA through NMD nor an alternative splicing through NAS. Moreover, immunocytochemical analysis in nasal epithelial cells revealed a significantly reduced amount of *CFTR* at the apical membrane providing a possible molecular explanation for the more severe phenotype observed in F508del/3905insT compound heterozygotes compared with F508del homozygotes. However, further experiments are needed to elucidate the fate of the 3905insT *CFTR* in the cell after its biosynthesis.

*European Journal of Human Genetics* (2010) 18, 212–217; doi:10.1038/ejhg.2009.140; published online 2 September 2009

**Keywords:** cystic fibrosis; *CFTR*; nonsense-mediated mRNA decay (NMD); nonsense-associated alternative splicing (NAS); genotype/phenotype correlation

## INTRODUCTION

Cystic fibrosis (CF; MIM# 219700) is one of the most common autosomal recessive disorders and occurs at a rate of 1 in 1600–3000 Caucasians. The classical symptoms include chronic obstructive pulmonary disease, exocrine pancreatic insufficiency, and elevation of sodium and chloride concentrations in the sweat.<sup>1,2</sup> Moreover, most males with CF present with infertility as a result of congenital bilateral absence of the vas deferens.<sup>3,4</sup> CF is caused by mutations in the *CFTR* transmembrane conductance regulator (*CFTR*; MIM# 602421) gene.<sup>5,6</sup> It encodes a protein that functions as a cAMP-activated chloride channel at the apical membrane of epithelial cells.<sup>7</sup> So far, over 1600 mutations and polymorphisms have been described in the *CFTR* gene (Cystic Fibrosis Genetic Analysis Consortium; www.genet.sickkids.on.ca/cfr). The genotype–phenotype relation in CF is known to be very complex. Some phenotypic features are closely determined by the genotype in an essentially monogenic manner, whereas others are strongly influenced by both modifying genetic factors and the environment leading to the realization that a disease phenotype is the sum of variable clinical components that arise from different molecular mechanisms of underlying mutations as well as from influences and interplay of many other factors. Thus, this variability in disease manifestation and severity can even be observed among patients carrying the same genotype. In a former study, mutation analysis has revealed that the frameshift mutation 3905insT (c.3773\_3774insT)

in exon 20 accounts for the second most common (4.8%) *CFTR* mutation in the Swiss population.<sup>8</sup> The mutation has also been identified to be a common *CFTR* mutation in the Amish (16.7%) and Acadian (14.3%) population in Pennsylvania and Louisiana, respectively, which are known to have a Swiss descent (Cystic Fibrosis Genetic Analysis Consortium; www.genet.sickkids.on.ca/cfr). Earlier studies based on clinical parameters have shown that the 3905insT mutation is associated with a severe phenotype.<sup>9–12</sup> The insertion of an additional thymidine in exon 20 leads to a premature termination codon (PTC) in the same exon. It is well known that PTCs can activate the nonsense-mediated mRNA decay (NMD). This control mechanism detects and degrades mRNAs bearing PTCs, thereby preventing the generation of truncated proteins that may be harmful for the cell.<sup>13,14</sup> During the NMD process, both splicing and translation have a crucial function for the distinction between normal stop codons and PTCs. Until recently, NMD was thought to be triggered when the PTC is located >50–55 nucleotides upstream of the last exon–exon junction (EEJ).<sup>15,16</sup> However, there is growing evidence that it is rather the physical distance between the PTC and the poly(A) tail, which determines whether a PTC-containing mRNA is an NMD substrate or not.<sup>17,18</sup> Another mechanism that has recently been associated with PTCs is nonsense-associated alternative splicing (NAS). In contrast to NMD, NAS activates alternative splicing that leads to the removal of the faulty PTC.<sup>14,19</sup>

<sup>1</sup>Department of Paediatrics, Division of Human Genetics, University of Bern, Bern, Switzerland and <sup>2</sup>Department of Internal Medicine, Institute of Medical Genetics, University of Zürich, Schwerzenbach, Switzerland

\*Correspondence: Professor S Gallati, Department of Paediatrics, Division of Human Genetics, Children's University Hospital, Inselspital, Bern, 3010, Switzerland.

Tel: +413 1632 9494; Fax: +413 1632 9484; E-mail: sabina.gallati@insel.ch

Received 26 January 2009; revised 29 June 2009; accepted 30 June 2009; published online 2 September 2009

In this work, we have applied RT-PCR and semi-quantitative analysis to investigate the possible molecular consequences of the frameshift mutation 3905insT at transcript level by analyzing the involvement of NMD and NAS. In addition, we have also performed immunocytochemistry to determine the subcellular localization of the presumably truncated CFTR protein in nasal epithelial cells from patients carrying the mutation.

## MATERIALS AND METHODS

### Mutation nomenclature

Nucleotide (cDNA) numbering is based on the CF mutation database (<http://www.genet.sickkids.on.ca/cfr/>) using +1 as the first nucleotide of the reference sequence (GenBank NM\_000492.2). Mutation nomenclature according to international recommendations ([www.hgvs.org/mutnomen](http://www.hgvs.org/mutnomen)) using +1 as the A of the ATG start codon in the reference sequence is indicated in brackets.

### Patients

A total of 16 CF patients seen at the Department of Pediatrics, Inselspital, Berne, Switzerland were selected for this study. Ten patients carried the F508del (p.Phe508del) mutation on one allele and the 3905insT (c.3773\_3774insT) mutation on the other. Two patients carried the 3905insT (c.3773\_3774insT) mutation on one allele and the P5L (p.Pro5Leu) or the Q39X (p.Gln39X) mutation, respectively, on the other allele. One patient was homozygous for the 3905insT (c.3773\_3774insT) mutation and three patients were homozygous for the F508del (p.Phe508del) mutation. All patients fulfilled the consensus for classic CF.<sup>1,2</sup> Informed consent was obtained from all subjects and the local ethics committee approved the study.

### Genomic analysis

An EDTA blood sample for DNA analysis was obtained from patients and controls. Mutation screening of the entire coding sequence of the *CFTR* gene (including the 27 exons, exon–intron boundaries, parts of introns 11 and 19, the promoter region, and the polymorphic sequence 1342-34(TG)10-13(T)3-9 (c.1210-34(TG)10-13(T)3-9) in intron 8) was performed using single-strand conformation polymorphism/heteroduplex analysis with a detection rate of 97.5%.<sup>20</sup> DNA samples presenting with aberrant band patterns on either single or double strands were directly sequenced in both directions.

### Cell culture and tissue collection

Human lymphoblastoid cells were prepared by Epstein–Barr virus immortalization of patients' blood lymphocytes. Tissue from the colon and the skin were collected under sterile environment during a surgical intervention. After collection, the tissue was immediately snap frozen and subsequently stored at  $-80^{\circ}\text{C}$ .

### RNA isolation

For EBV-transformed lymphocytes, total cellular RNA was isolated with the Aurum Total RNA Mini Kit (Bio-Rad, Reinach, Switzerland) according to the protocol for cultured cells. The samples were homogenized by passing the lysate 10 times through a 20-G needle fitted to a syringe. DNase treatment was performed according to the protocol. For skin and colon tissue, total RNA was isolated by first grinding frozen tissue in a mortar with liquid nitrogen and then following the protocol for animal tissue of the Aurum Total Mini Kit. The samples were homogenized by passing the lysate 10 times through a 20-G needle fitted to a syringe. DNase treatment was performed according to the protocol. RNA concentration was measured using a NanoDrop spectrophotometer (NanoDrop Technologies, Wilmington, DE, USA). Until further processing, the RNA was stored in the presence of 40 Units RNase Inhibitor (Roche, Rotkreuz, Switzerland) at  $-20^{\circ}\text{C}$ .

### RT-PCR

A cDNA fragment encompassing exons 19–24 was amplified in a Perkin Elmer 9700 thermocycler by one-step RT-PCR using the SuperScript one-step RT-PCR kit for long templates (Invitrogen, Basel, Switzerland). Reverse transcription was performed at  $55^{\circ}\text{C}$  for 30 min. After polymerase activation at  $95^{\circ}\text{C}$  for 2 min, 40 cycles of PCR with denaturation at  $95^{\circ}\text{C}$  for 15 s, primer annealing at  $55^{\circ}\text{C}$  for 30 s, and extension at  $68^{\circ}\text{C}$  for 1 min, a final extension at

$68^{\circ}\text{C}$  for 3 min was carried out. The primer pairs used were 5'-ATA CAC AGA AGG TGG AAA TGC, reverse primer 5'-GTC CCA TGT CAA CAT TTA TGC TGC T. Product identity was confirmed by sequencing on an ABI Prism 3100 Genetic Analyzer (Applied Biosystems, Warrington, UK).

### Agarose gel electrophoresis

A total of 3  $\mu\text{l}$  of the amplification product was mixed with 7  $\mu\text{l}$  of water and 2  $\mu\text{l}$  of loading buffer. The mixture was loaded onto a 2% agarose gel and electrophoresis was performed at 120 V for 2 h. Visualization of the bands was achieved using ethidium bromide and the UV imaging system UviDoc (Witec AG, Littau, Switzerland).

### RNA analysis

A cDNA fragment encompassing exons 9–10 was amplified with the one-step RT-PCR kit (Qiagen, Basel, Switzerland) in a LightCycler system (Roche, Basel, Switzerland) with SYBR-Green I to monitor fluorescence increase. Total RNA from a control subject (wild-type, wt) and from a patient homozygous for the F508del mutation was reverse transcribed at  $50^{\circ}\text{C}$  for 30 min. After polymerase activation at  $95^{\circ}\text{C}$  for 15 min, 45 cycles of PCR with denaturation at  $95^{\circ}\text{C}$  for 0 s, and primer annealing at  $58^{\circ}\text{C}$  for 25 s, an extension at  $72^{\circ}\text{C}$  for 15 s was carried out using the forward primer 5'-CAGTTTCTCTGGATTATGCTT (exon 10) and the reverse primer 5'-CTTGAGATGTCCTCTCTAGTTG (junction exons 10 and 11) yielding a cDNA of 120 bp for the wt and 117 bp for the F508del. Fluorescence was measured at the end of the elongation step. All reactions were performed in duplicates, and melting curve analysis and sequencing ensured product identity. To compare amplification efficiency, wt and F508del cDNA was purified using the QIAquick purification kit (Qiagen). Subsequently,  $10^6$ ,  $10^5$ ,  $10^4$ ,  $10^3$ , and  $10^2$  copies/ $\mu\text{l}$  cDNA standards were prepared by serial dilution. The LightCycler Software 3.5 (Roche) automatically generated a standard curve for each cDNA after performing amplification on the LightCycler with 2  $\mu\text{l}$  of each standard under the same conditions mentioned before.

mRNA obtained from F508del/3905insT EBV-transformed lymphocytes was used to perform real-time RT-PCR under the same conditions as described before in this section using the same primer sequences, but with the forward primer being labeled with the fluorescence dye HEX. All reactions were performed in triplicates and RT-PCR was stopped in the exponential phase by monitoring SYBR-Green I fluorescence. A total of 0.5  $\mu\text{l}$  of the amplification product were then subjected to capillary electrophoresis on an ABI Prism 3100 Genetic Analyzer (Applied Biosystems). The GeneScan-500 ROX Size Standard (Applied Biosystems) was used as an internal standard to determine the size of the amplified fragments. Quantification was performed using the GeneMapper 3.5 software (Applied Biosystems) by comparing the fluorescence peak area of the 3905insT (120 bp) cDNA relative to the one corresponding to the F508del (117 bp) cDNA.

### Immunocytochemistry

Lab-Tek II Multichamber slides (Nalge Nunc International, Naperville, IL, USA) were treated with 300  $\mu\text{l}$  of freshly prepared 0.01% (w/v) poly-L-lysine (Sigma-Aldrich, Buchs, Switzerland) solution at  $37^{\circ}\text{C}$  for 30 min. The slides were then washed twice with water for 5 min, dried, and eventually stored at  $4^{\circ}\text{C}$  until further use. Epithelial cells were collected by nasal brushing. Interdental brushes with 2.5–3 mm bristles (ParoIsola, Thalwil, Switzerland) were used to scrape the inferior turbinates of both nostrils, using two brushes for each side. Cellular material was removed from the brushes by passing the brush through a 100- $\mu\text{l}$  pipette tip with a sectioned tip. The cell suspension was then centrifuged at 5000 rpm for 5 min and the supernatant was removed leaving some liquid over the pellet. Fixation was performed with ice-cold 4% (v/v) formaldehyde/3.7% (w/v) sucrose solution in PBS for 30 min at  $4^{\circ}\text{C}$ . The cell suspension was then centrifuged at 3000 rpm for 5 min and the formaldehyde/sucrose solution was completely removed. The cells were resuspended in cold PBS and transferred to the wells of the multichamber slide. After centrifugation at 200 g for 5 min, the liquid was removed from the wells and the samples were air dried for at least 10 min. Permeabilization was performed with PBS+0.1% Triton X-100 for 10 min at RT. The cells were washed twice with PBS and then blocked with PBS+2% normal goat serum (NGS)

(Sigma-Aldrich)+1% BSA (Sigma-Aldrich) for at least 1 h at RT. After five washes with PBS of 5 min each at RT, the cells were incubated over night (16 h) at 4°C with one of the two primary antibodies MAB3480 (clone M3A7 against C-terminus) and MAB3484 (clone L12B4 against R region) (Chemicon, Hofheim, Germany) diluted 1:100 in PBS+2% NGS+1% BSA. The cells were then washed five times with PBS for 5 min and incubated for 1 h at RT with an Alexa 488 fluor-conjugated secondary antibody (Molecular Probes goat anti-mouse) (Invitrogen) diluted 1:200 in PBS+2% NGS+1% BSA. Staining of the Golgi was performed with Alexa 594 fluor-conjugated wheat germ agglutinin from Molecular Probes (Invitrogen). After five washes of 5 min each with PBS at RT, cell nuclei were stained using DAPI from Molecular Probes (Invitrogen). Finally, cells were mounted with ProLong AntiFade Kit from Molecular Probes (Invitrogen). The stained cells were examined using a Nikon Eclipse E600 microscope and a Nikon Digital camera DXM1200.

## RESULTS

### The PTC introduced by the frameshift mutation 3905insT is insensitive to NMD and NAS

Four patients (P1–P4) carrying the 3905insT (c. 3773\_3774insT) mutation on one allele and the F508del (p.Phe508del) mutation on the other allele were selected to produce EBV-transformed lymphoblastoid cell cultures. Primers were designed to amplify a region containing the codon for F508del, yielding either a 120-bp fragment for the 3905insT allele or a 117-bp fragment for the F508del allele (Figure 1a). As even slight differences in amplification efficiency between the two fragments can considerably influence quantification results, standard curves were created by the LightCycler software for

both cDNAs. The obtained curves gave very similar slopes for both cDNAs, indicating that the two fragments were amplified with nearly the same efficiency (Figure 1b). Extracted RNA from cell cultures was then used to perform real-time RT–PCR on the LightCycler using HEX-labeled primers. Amplification was stopped in the exponential phase of the reaction and the amplification products were subsequently separated by capillary electrophoresis on an ABI3100 genetic analyzer. The GeneMapper software 3.5 was then used to integrate the area under the peaks corresponding to the 3905insT (120 bp) and the F508del cDNA (117 bp). As the F508del mutation is not expected to be affected by NMD, 3905insT transcript levels can be quantified relative to F508del levels. With the exception of P4 (26%), we obtained relative 3905insT mRNA proportions around 50% with values ranging between 45% (P3) and 54% (P1), indicating that the 3905insT allele produces nearly equal transcript levels compared with the F508del allele in P1, P2, and P3 (Figure 1c). These results strongly suggest that the PTC introduced by the frameshift mutation 3905insT does not cause instability of the corresponding mRNA through NMD.

To verify whether the 3905insT mutation is capable of triggering, an NAS response by inducing skipping of the PTC-containing exon, a region of 817 bp encompassing exons 19–24 was amplified by RT–PCR. Skipping of exon 20 would be expected to result in a 156-bp shorter fragment of 661 bp. However, neither the RNA from EBV lymphocytes (Figure 2a) nor the RNA from nasal epithelial cells carrying the 3905insT on one allele (Figure 2b) showed an indication for exon 20 skipping. The faint lower migrating fragments present for

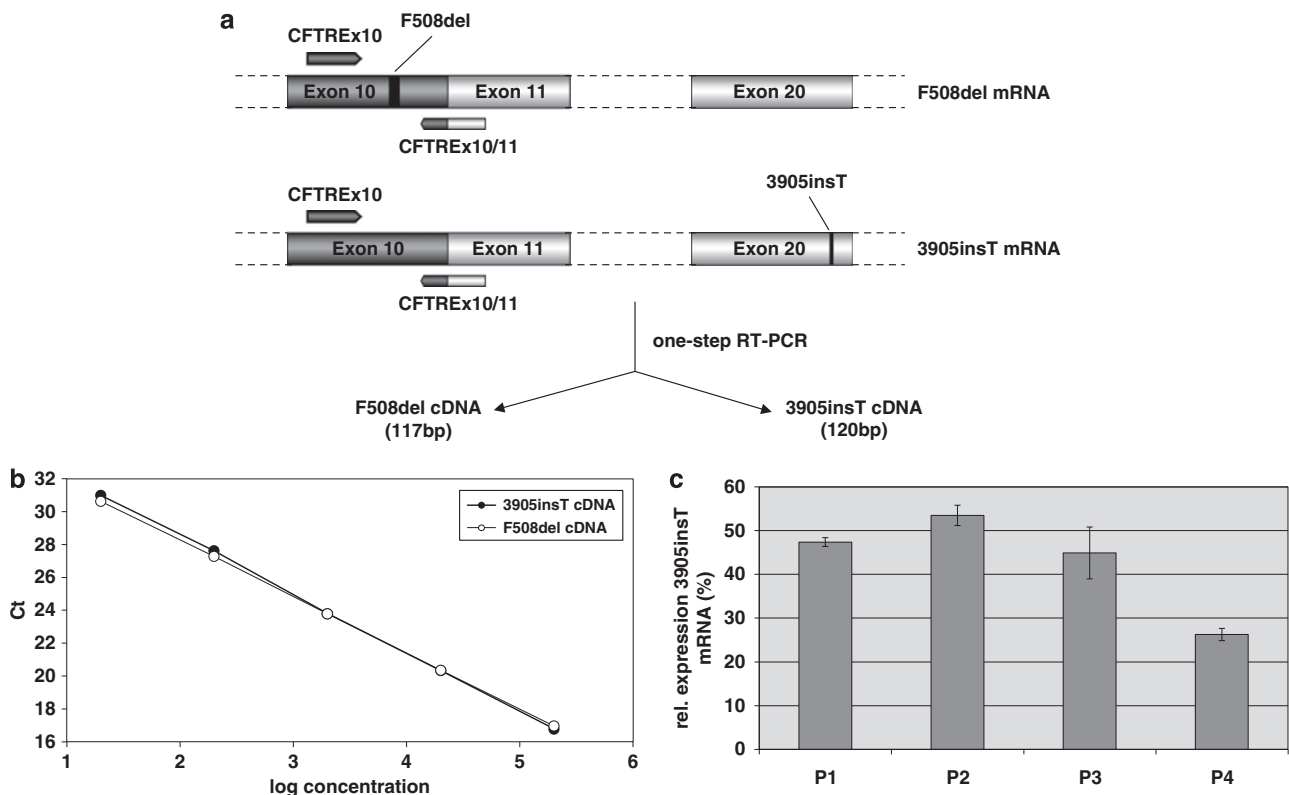


**Figure 1** (a) Schematic representation of the RT–PCR reaction that was performed to discriminate between the F508del and the 3905insT mRNA. Primers were designed to amplify the region containing the codon for phenylalanine at position 508 of the CFTR protein. RNA-specific amplification was ensured by the binding of the reverse primer to the exon 10/11 junction. RT–PCR with these primers yielded a 120-bp cDNA fragment for the 3905insT mRNA and a 3-bp shorter cDNA of 117 bp for the F508del mRNA. (b) Comparable standard curves obtained with 3905insT (black dots) and F508del (white dots) cDNA standards show that both alleles are amplified with the same efficiency. (c) Allele-specific quantification of 3905insT mRNA in EBV-transformed lymphocytes. The indicated mRNA proportion was calculated relative to the F508del mRNA. Error bars indicate the corresponding standard error (SE).

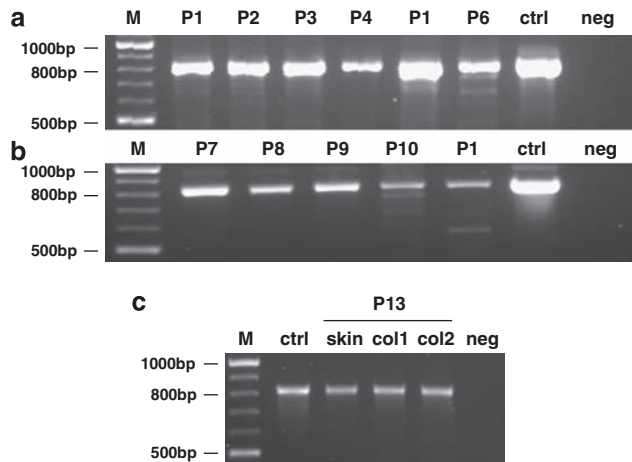


**Figure 2** RT-PCR results obtained for the amplification of a region encompassing exons 19–24 of the *CFTR* mRNA derived from EBV-transformed lymphocytes of F508del/3905insT patients (a), nasal epithelial cells of F508del/3905insT patients (b), and from skin and colon samples of a 3905insT/3905insT patient (c). The reaction yields a cDNA fragment of 661 bp if exon 20 is skipped because of the presence of the PTC in this exon, and a cDNA of 817 bp in case no alternative splicing occurs.

some patients are either because of PCR artifacts deriving from mispriming or to transcripts arising from improper splice-site recognition during splicing. Similarly, RNA obtained from skin and colon tissue of a 3905insT homozygous patient revealed no alternative splicing of exon 20 (Figure 2c). Sequencing confirmed that the cDNA obtained from lymphocytes and nasal epithelial cells was derived from 3905insT transcripts of the compound-heterozygous patients (Figure 2a and b) and the homozygous patient (Figure 2c) (data not shown). These results further strengthen the evidence that transcripts carrying the 3905insT mutation are neither degraded through NMD nor alternatively spliced by NAS.

### Subcellular localization of 3905insT *CFTR*

On the basis of the obtained results, we assumed that the undegraded mRNA derived from the 3905insT allele would lead to the generation of a truncated protein. To analyze the possible intracellular fate of this truncated *CFTR* protein, immunocytochemistry was performed with nasal epithelial cells collected from three CF F508del/3905insT compound heterozygotes and from three F508del homozygous patients. Two different *CFTR* antibodies were used, which recognize the R region and the C-terminus of *CFTR*, respectively. Both antibodies were able to detect *CFTR* at the apical membrane (Figure 3a) in around 55% of the analyzed nasal epithelial cells derived from controls (Table 1). Although MAB3484 (R region) distinctively stained the apical region in most cells, MAB3480 (C-terminal) usually also showed a more diffuse labeling, including the subapical region (arrowheads, Figure 3a). Similarly, in cells from F508del homozygotes, both antibodies were able to detect *CFTR* at the apical membrane, however, in a reduced number of cells (Table 1) and with weaker apical signals as in wt cells (Figure 3b, arrowheads). Moreover, in some cells, a *CFTR*-unspecific intracellular structure was detected, which co-localized with the Golgi compartment (Figure 3b, arrows). This unspecific staining has earlier been reported in another study in which these two antibodies were also used to detect *CFTR* in nasal epithelial cells.<sup>21</sup> In contrast to wt and F508del homozygous cells, we observed a significantly reduced amount of nasal epithelial cells from F508del/3905insT compound heterozygotes with an apical staining as

compared with F508del homozygotes (Figure 3c; Table 1,  $P \leq 0.05$ ). Again, some cells showed the unspecific Golgi-like intracellular structure (Figure 3c, arrows). Unfortunately, the only 3905insT homozygous patient in our study was a newborn, and we thus had no possibility to perform a nasal brushing to confirm these findings in 3905insT homozygous cells.

### DISCUSSION

The frameshift mutation 3905insT (c. 3773\_3774insT) is one of the most common *CFTR* mutations in the Swiss population<sup>8</sup> and has been associated with a severe phenotype.<sup>9–12</sup> The mutation is characterized by the introduction of a PTC in exon 20 of the *CFTR* gene. PTCs can be recognized by the so-called NMD, which degrades transcripts bearing such PTCs thereby preventing the formation of a truncated protein.<sup>14</sup> It has also been proposed that PTCs can be targeted by another mechanism termed NAS, in which the exon containing the PTC is excluded from the mRNA through alternative splicing reducing the levels of full-length *CFTR* transcripts.<sup>22</sup> Performing a combination of real-time RT-PCR and fragment analysis, we could show that the 3905insT mRNA is insensitive to complete degradation by NMD (Figure 1c). Three out of four patients showed transcript levels of around 50%, whereas P4 presented with levels of 26% raising awareness of additional complex mechanisms such as individual and tissue-specific expression and/or stability of mRNAs.<sup>23</sup> The lack of degradation by NMD was further confirmed by RT-PCR amplification, in which we were able to detect 3905insT cDNA from skin and colon samples of a 3905insT homozygous patient (Figure 2c). Moreover, we present evidence that 3905insT transcripts are not subject to alternative splicing by NAS in different tissues of 3905insT carriers (Figure 2). To our knowledge, this is the first *CFTR* frameshift mutation that has extensively been analyzed for the influence of NMD, and additionally of NAS. Furthermore, it is also the first report of a *CFTR* frameshift mutation that constitutes an exception to the ‘50–55 boundary rule’, which states that NMD is triggered whenever a PTC is located >50–55 nucleotides upstream of the last EEJ.<sup>15,16</sup> There is a growing number of mutations that have been reported to be insensitive to NMD<sup>24–29</sup> supporting a novel model in which the physical distance between the PTC and the poly(A) tail is at least as crucial as the distance between the PTC and the last EEJ.<sup>30</sup> This model might explain the resistance of 3905insT mRNA to NMD, particularly when considering the relative proximity of the emerging PTC to the poly(A) tail.

Aberrant proteins produced in the endoplasmic reticulum (ER) are recognized and then destroyed by a process termed as ER-associated protein degradation (ERAD).<sup>31</sup> It is well established that F508del *CFTR* is degraded because of a misfolding of the protein that results in an almost complete lack of protein at the plasma membrane. In spite of the degradation, some F508del protein can reach the apical membrane and function as a chloride channel.<sup>32</sup> Several studies have shown that the presence of this residual *CFTR* activity correlates with a milder CF phenotype in F508del homozygotes.<sup>33–35</sup> The findings that 3905insT mRNA was insensitive to NMD despite harboring a PTC, led us to the assumption that this mRNA would cause the formation of a truncated protein. To assess the fate of this truncated protein in the cell, we performed immunocytochemical analysis in nasal epithelial cells collected from the patients. In contrast to wt and F508del/F508del cells, in which the *CFTR* protein could be detected at the apical membrane (Figure 3a), apical *CFTR* staining was significantly reduced in nasal epithelial cells derived from F508del/3905insT compound-heterozygous patients (Figure 3c; Table 1). These immunocytochemical results confirmed earlier findings showing that a reduced

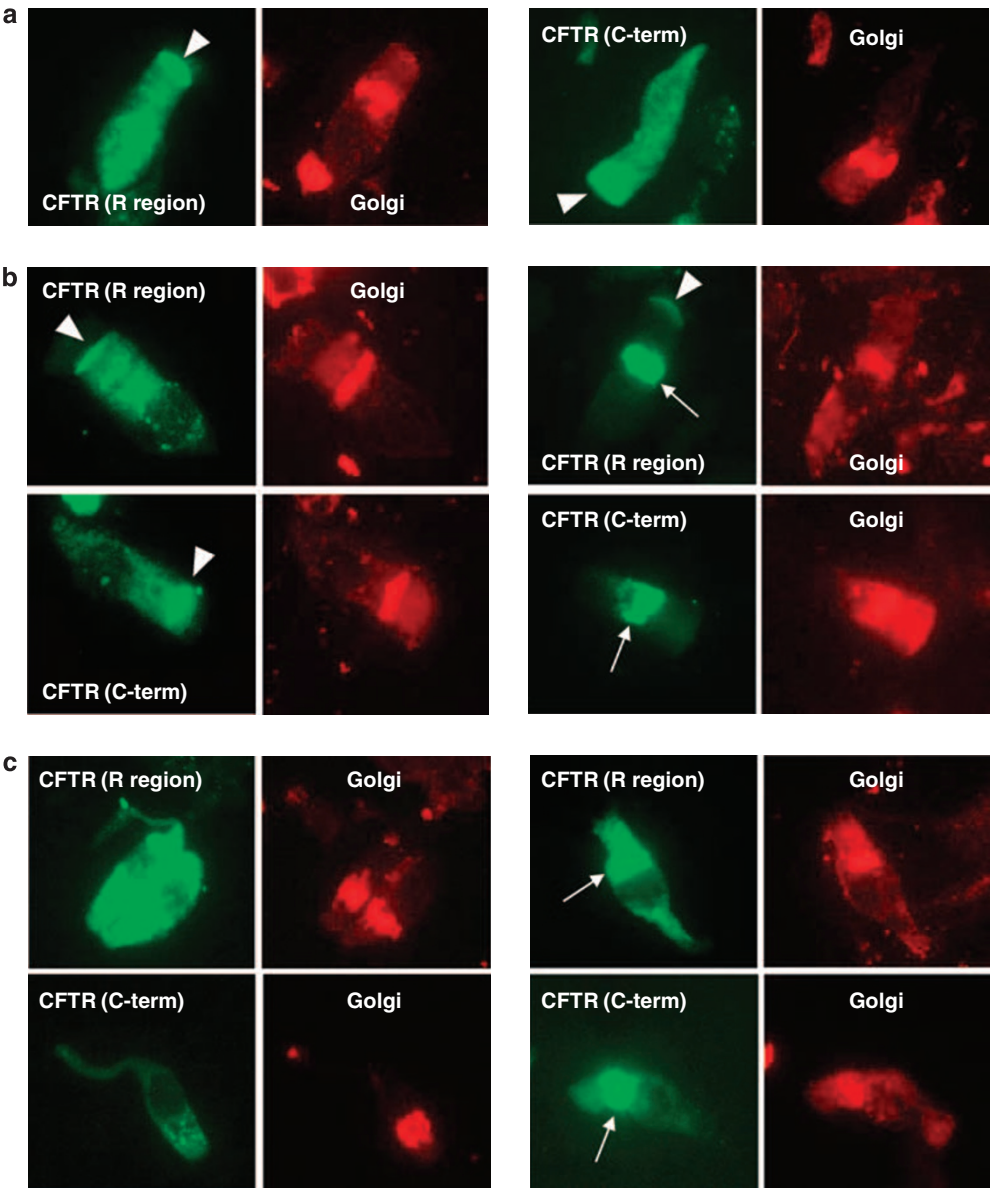


**Figure 3** Immunocytochemical analysis of CFTR in nasal epithelial cells derived from controls (a), from F508del/F508del patients (b), and from F508del/3905insT patients (c). CFTR was detected using either an antibody directed against the C-terminal or the R region of the protein, and the Golgi compartment was stained using wheat germ agglutinin. Arrowheads indicate CFTR localized at the apical membrane of the cells, whereas arrows display an unspecific Golgi-like structure earlier mentioned in the literature.

number of cells from F508del homozygous patients have apically localized CFTR (Figure 3b).<sup>21,36,37</sup> Recent studies indicated that the CFTR C-terminus is not required for the biosynthesis and plasma membrane targeting of CFTR, but indispensable for maintaining the stability of the protein.<sup>38</sup> Benharouga *et al.*<sup>39</sup> could also show that an ERAD-similar mechanism involving the proteasome-ubiquitin pathway may be responsible for the faster turnover and the short residence time at the apical membrane of truncated CFTR. This faster recycling rate of truncated proteins may provide an explanation for the reduced amount of 3905insT CFTR at the apical membrane. However, it has to be noted that the above-mentioned studies investigated protein truncations shorter than 98 amino acids. Owing to the expected large truncation of 216 residues in the 3905insT CFTR, we assume that it is very likely that degradation occurs through the conventional ERAD

**Table 1** Proportion of cells with apically localized CFTR

	Mean (%)	Samples
Wild type	55	2
F508del/F508del	38	3
F508del/3905insT	8	3

pathway. Another hypothesis for the complete lack of CFTR at the apical membrane would be that there is an interaction between the F508del and the 3905insT protein somehow hindering each other to reach the plasma membrane. In conclusion, the reduced presence of CFTR protein at the apical membrane may provide a possible explanation for the more severe phenotype observed in 3905insT/

F508del compound-heterozygous patients *versus* F508del homozygous patients, in which at least some CFTR can escape the ER, reach the apical membrane, and function as a chloride channel. However, further experiments need to be performed to see whether the truncated 3905insT protein is degraded before reaching the apical membrane, whether it is quickly recycled after reaching the membrane, or whether there is an interaction between the 3905insT and the F508del CFTR protein interfering with the transport to the apical membrane.

## ACKNOWLEDGEMENTS

We are indebted to the patients and clinicians involved for their cooperation and collaboration and thank André Eble for EBV transformation of the lymphocytes. This work was funded by grants from the Swiss National Foundation (3200-066767.01 to SG, 310000-112652 to SG).

- Rosenstein BJ, Cutting GR: The diagnosis of cystic fibrosis: a consensus statement. Cystic Fibrosis Foundation Consensus Panel. *J Pediatr* 1998; **132**: 589–595.
- Knowles MR, Durie PR: What is cystic fibrosis? *N Engl J Med* 2002; **347**: 439–442.
- Chillon M, Casals T, Mercier B *et al*: Mutations in the cystic fibrosis gene in patients with congenital absence of the vas deferens. *N Engl J Med* 1995; **332**: 1475–1480.
- Zielenski J, Patrizio P, Corey M *et al*: CFTR gene variant for patients with congenital absence of vas deferens. *Am J Hum Genet* 1995; **57**: 958–960.
- Riordan JR, Rommens JM, Kerem B *et al*: Identification of the cystic fibrosis gene: cloning and characterization of complementary DNA. *Science* 1989; **245**: 1066–1073.
- Kerem B, Rommens JM, Buchanan JA *et al*: Identification of the cystic fibrosis gene: genetic analysis. *Science* 1989; **245**: 1073–1080.
- Collins FS: Cystic fibrosis: molecular biology and therapeutic implications. *Science* 1992; **256**: 774–779.
- Hergersberg M, Balakrishnan J, Bettecken T *et al*: A new mutation, 3905insT, accounts for 4.8% of 1173 CF chromosomes in Switzerland and causes a severe phenotype. *Hum Genet* 1997; **100**: 220–223.
- Liechti-Gallati S, Bonsall I, Malik N *et al*: Genotype/phenotype association in cystic fibrosis: analyses of the delta F508, R553X, and 3905insT mutations. *Pediatr Res* 1992; **32**: 175–178.
- Kraemer R, Birrer P, Liechti-Gallati S: Genotype-phenotype association in infants with cystic fibrosis at the time of diagnosis. *Pediatr Res* 1998; **44**: 920–926.
- Schibler A, Bolt I, Gallati S, Schoni MH, Kraemer R: High morbidity and mortality in cystic fibrosis patients compound heterozygous for 3905insT and deltaF508. *Eur Respir J* 2001; **17**: 1181–1186.
- Kraemer R, Baldwin DN, Ammann RA, Frey U, Gallati S: Progression of pulmonary hyperinflation and trapped gas associated with genetic and environmental factors in children with cystic fibrosis. *Respir Res* 2006; **7**: 138.
- Frischmeyer PA, Dietz HC: Nonsense-mediated mRNA decay in health and disease. *Hum Mol Genet* 1999; **8**: 1893–1900.
- Hentze MW, Kulozik AE: A perfect message: RNA surveillance and nonsense-mediated decay. *Cell* 1999; **96**: 307–310.
- Nagy E, Maquat LE: A rule for termination-codon position within intron-containing genes: when nonsense affects RNA abundance. *Trends Biochem Sci* 1998; **23**: 198–199.
- Maquat LE: Nonsense-mediated mRNA decay: splicing, translation and mRNP dynamics. *Nat Rev Mol Cell Biol* 2004; **5**: 89–99.
- Eberle AB, Stalder L, Mathys H, Orozco RZ, Muhlemann O: Posttranscriptional gene regulation by spatial rearrangement of the 3' untranslated region. *PLoS Biol* 2008; **6**: e92.
- Silva AL, Ribeiro P, Inacio A, Liebhaber SA, Romao L: Proximity of the poly(A)-binding protein to a premature termination codon inhibits mammalian nonsense-mediated mRNA decay. *RNA* 2008; **14**: 563–576.
- Maquat LE: NASTY effects on fibrillin pre-mRNA splicing: another case of ESE does it, but proposals for translation-dependent splice site choice live on. *Genes Dev* 2002; **16**: 1743–1753.
- Liechti-Gallati S, Schneider V, Neeser D, Kraemer R: Two buffer PAGE system-based SSCP/HD analysis: a general protocol for rapid and sensitive mutation screening in cystic fibrosis and any other human genetic disease. *Eur J Hum Genet* 1999; **7**: 590–598.
- Carvalho-Oliveira I, Efthymiadou A, Malho R *et al*: CFTR localization in native airway cells and cell lines expressing wild-type or F508del-CFTR by a panel of different antibodies. *J Histochem Cytochem* 2004; **52**: 193–203.
- Wang J, Chang YF, Hamilton JI, Wilkinson MF: Nonsense-associated altered splicing: a frame-dependent response distinct from nonsense-mediated decay. *Mol Cell* 2002; **10**: 951–957.
- Linde L, Boelz S, Neu-Yilik G, Kulozik AE, Kerem B: The efficiency of nonsense-mediated mRNA decay is an inherent character and varies among different cells. *Eur J Hum Genet* 2007; **15**: 1156–1162.
- Romao L, Inacio A, Santos S *et al*: Nonsense mutations in the human beta-globin gene lead to unexpected levels of cytoplasmic mRNA accumulation. *Blood* 2000; **96**: 2895–2901.
- Asselta R, Duga S, Spena S *et al*: Congenital afibrinogenemia: mutations leading to premature termination codons in fibrinogen A alpha-chain gene are not associated with the decay of the mutant mRNAs. *Blood* 2001; **98**: 3685–3692.
- Perrin-Vidol L, Sinilnikova OM, Stoppa-Lyonnet D, Lenoir GM, Mazoyer S: The nonsense-mediated mRNA decay pathway triggers degradation of most BRCA1 mRNAs bearing premature termination codons. *Hum Mol Genet* 2002; **11**: 2805–2814.
- Danckwardt S, Neu-Yilik G, Thermann R, Frede U, Hentze MW, Kulozik AE: Abnormally spliced beta-globin mRNAs: a single point mutation generates transcripts sensitive and insensitive to nonsense-mediated mRNA decay. *Blood* 2002; **99**: 1811–1816.
- Denecke J, Kranz C, Kemming D, Koch HG, Marquardt T: An activated 5' cryptic splice site in the human ALG3 gene generates a premature termination codon insensitive to nonsense-mediated mRNA decay in a new case of congenital disorder of glycosylation type Id (CDG-Id). *Hum Mutat* 2004; **23**: 477–486.
- Neerman-Arbez M, Germanos-Haddad M, Tzanidakis K *et al*: Expression and analysis of a split premature termination codon in FGG responsible for congenital afibrinogenemia: escape from RNA surveillance mechanisms in transfected cells. *Blood* 2004; **104**: 3618–3623.
- Stalder L, Muhlemann O: The meaning of nonsense. *Trends Cell Biol* 2008; **18**: 315–321.
- Klausner RD, Sitia R: Protein degradation in the endoplasmic reticulum. *Cell* 1990; **62**: 611–614.
- Kopito RR: Biosynthesis and degradation of CFTR. *Physiol Rev* 1999; **79**: S167–S173.
- Sermet-Gaudelus I, Vallee B, Urbin I *et al*: Normal function of the cystic fibrosis conductance regulator protein can be associated with homozygous (Delta)F508 mutation. *Pediatr Res* 2002; **52**: 628–635.
- Bronsveld I, Mekus F, Bijman J *et al*: Chloride conductance and genetic background modulate the cystic fibrosis phenotype of Delta F508 homozygous twins and siblings. *J Clin Invest* 2001; **108**: 1705–1715.
- Thomas SR, Jaffe A, Geddes DM, Hodson ME, Alton EW: Pulmonary disease severity in men with deltaF508 cystic fibrosis and residual chloride secretion. *Lancet* 1999; **353**: 984–985.
- Penque D, Mendes F, Beck S *et al*: Cystic fibrosis F508del patients have apically localized CFTR in a reduced number of airway cells. *Lab Invest* 2000; **80**: 857–868.
- Dorner RL, McNeilly CM, Morris MR *et al*: Localisation of wild-type and DeltaF508-CFTR in nasal epithelial cells. *Pflugers Arch* 2001; **443** (Suppl 1): S117–S120.
- Haardt M, Benharouga M, Lechardeur D, Kartner N, Lukacs GL: C-terminal truncations destabilize the cystic fibrosis transmembrane conductance regulator without impairing its biogenesis. A novel class of mutation. *J Biol Chem* 1999; **274**: 21873–21877.
- Benharouga M, Haardt M, Kartner N, Lukacs GL: COOH-terminal truncations promote proteasome-dependent degradation of mature cystic fibrosis transmembrane conductance regulator from post-Golgi compartments. *J Cell Biol* 2001; **153**: 957–970.